

# Responses of infrared-sensitive tectal units of the pit viper *Crotalus atrox* to moving objects

Felix Kaldenbach<sup>1</sup> · Horst Bleckmann<sup>1</sup> · Tobias Kohl<sup>2</sup>

Received: 4 May 2015 / Revised: 22 December 2015 / Accepted: 4 February 2016 / Published online: 23 February 2016  
© Springer-Verlag Berlin Heidelberg 2016

**Abstract** Rattlesnakes perceive IR radiation with their pit organs. This enables them to detect and strike towards warm-blooded prey even in the dark. In addition, the IR sense allows rattlesnakes to find places for thermoregulation. Animate objects (e.g., prey) tend to move and thus cause moving IR images across the pit membrane. Even when an object is stationary, scanning head movements of rattlesnakes will result in moving IR images across the pit membrane. We recorded the neuronal activity of IR-sensitive tectal neurons of the rattlesnake *Crotalus atrox* while stimulating the snakes with an IR source that moved horizontally at various velocities. As long as object velocity was low (angular velocity of  $\sim 5^\circ/\text{s}$ ) IR-sensitive tectal neurons hardly showed any responses. With increasing object velocity though, neuronal activity reached a maximum at  $\sim 50^\circ/\text{s}$ . A further increase in object velocity up to  $\sim 120^\circ/\text{s}$  resulted in a slight decrease of neuronal activity. Our results demonstrate the importance of moving stimuli for the snake's IR detection abilities: in contrast to fast moving objects, stationary or slowly moving objects will not be detected when the snake is motionless, but might be detected by scanning head movements.

**Keywords** Infrared reception · Rattlesnake · Velocity · Motion · Tectum opticum

## Abbreviations

IR Infrared  
LTDD Nucleus descendens lateralis nervi trigemini  
RC Nucleus reticularis caloris  
RF Receptive field

## Introduction

Pitvipers (Crotalinae), most boas (Boinae) and pythons (Pythoninae) are sensitive to infrared (IR) radiation (Noble and Schmidt 1937; de Cock Buning et al. 1981a, b). IR receptors, called pit organs, enable these snakes to detect and localize prey (Noble and Schmidt 1937; Kardong and Mackessy 1991; Chen et al. 2012), to avoid predators (Van Dyke and Grace 2010) and to select places for thermoregulation (Krochmal and Bakken 2003). Each pit organ of crotaline snakes (e.g., rattlesnakes) consists of a 10–15  $\mu\text{m}$  thick membrane, suspended within a cavity located between the eye and the nostril on either side of the snake's head (Lynn 1931; Noble and Schmidt 1937; Bullock and Fox 1957). In contrast to the photochemical transduction process known from visual cells, pit organs function like bolometers, i.e., thermal radiation is absorbed by the pit membrane, increasing the pit membrane temperature. This temperature change is detected by fibers of the trigeminal nerve apparently by means of heat sensitive TRPA1-channels (Gracheva et al. 2010).

In rattlesnakes, IR-sensitive trigeminal nerve fibers project ipsilaterally to the nucleus descendens lateralis nervi trigemini (LTDD) of the hindbrain (Molenaar 1974;

✉ Tobias Kohl  
tobias.kohl@wzw.tum.de

Felix Kaldenbach  
felixkaldenbach@uni-bonn.de

<sup>1</sup> Institute of Zoology, Rheinische Friedrich-Wilhelms-University Bonn, Poppelsdorfer Schloss, Meckenheimer Allee 169, 53115 Bonn, Germany

<sup>2</sup> Chair of Zoology, Technical University of Munich, Liesel-Beckmann-Str. 4, 85354 Freising-Weißenstephan, Germany

Schroeder and Loop 1976; Kohl et al. 2014). Efferents of the LTTD project to the ipsilateral nucleus reticularis caloris (RC) which projects to the contralateral optic tectum (Gruberg et al. 1979; Newman et al. 1980; Kishida et al. 1980). In the tectum, IR information merges with visual information (Hartline et al. 1978; Newman and Hartline 1981).

So far, in almost all electrophysiological studies, the pit organs of rattlesnakes were stimulated by a stationary IR source and with an abrupt stimulus onset (Terashima et al. 1968; Harris and Gamow 1971; de Cock Buning 1983; Moiseenkova et al. 2003). This type of stimulus induces a rapid temperature increase of the pit membrane at stimulus onset and a subsequent rapid temperature decrease at stimulus offset. In contrast, natural animate IR sources (e.g., prey) often move, thereby causing temporal temperature modulation of the pit membrane. Non-moving prey (or predators) and hiding places suitable for thermoregulation (Krochmal and Bakken 2003) are also detected by IR-sensitive snakes, most likely by scanning head movements. These movements cause a similar temporal and spatial temperature modulation of the pit membrane as moving prey. Thus, although IR stimuli with abrupt onsets are well suited to stimulate IR receptors, they may not be relevant under natural conditions.

Behavioral studies show that blindfolded rattlesnakes and pythons predominantly respond to moving IR sources (Noble and Schmidt 1937; Ebert and Westhoff 2006). This finding is supported by electrophysiological studies that describe strong, but non-quantified neuronal responses to moving IR sources (Goris and Nomoto 1967; Goris and Terashima 1973; Terashima and Goris 1976; Hartline et al. 1978). However, these studies lack a systematic investigation of the relation between stimulus velocity and neuronal activity. Besides velocity, movement direction is also an important stimulus parameter. Directional sensitive tectal IR units have been recorded from rattlesnakes (Hartline et al. 1978), but these findings were not confirmed in other studies (Terashima and Goris 1976). In the present study, we investigated the responses of tectal units to moving IR sources of different velocity and movement direction.

## Materials and methods

### Experimental animals

A total of 19 western diamondback rattlesnakes (*Crotalus atrox*, Baird and Girard 1853) were used. The age of the snakes ranged from 6 to 24 months (snout-vent length:  $67 \pm 14$  cm; weight:  $150 \pm 94$  g). Snakes were maintained in a snake room, on a 12:12 h light:dark cycle, 22–30 °C

temperature range and a diet of pre-killed mice. Access to water was ad libitum.

### Anesthesia

Prior to surgery, snakes were anesthetized in an air-tight plastic box (20 × 20 × 10 cm) into which 1 ml of isoflurane (Actavis Deutschland GmbH & Co. KG, München-Riem, Germany) was injected. After 30–45 min the snakes no longer responded to a tail-pinch. Snakes were intubated with a flexible plastic catheter (1.0 × 130 mm; Buster Cat Catheter, Jørgen Kruuse A/S, Langeskov, Denmark) ventilated with carbogen gas (95 % O<sub>2</sub>, 5 % CO<sub>2</sub>; 25 ml/h per gram body weight; Air Liquide Deutschland GmbH, Düsseldorf, Germany) that was enriched with Isoflurane (2 %) by a veterinary vaporizer (Isotec-3, Völker GmbH, Kaltenkirchen, Germany). A deep level of anesthesia was maintained throughout all experiments.

### Surgical procedures

All surgical procedures were performed under a dissecting microscope (M3Z, Wild, Heerbrugg, Switzerland). The skin on top of the head was excised to expose the parietal bones that cover the optic tectum. Parietal bones were milled with a burr (Minimot 40/E, Proxxon GmbH, Niersbach, Germany) until only a thin layer remained. To expose the optic tectum this layer as well as the meninges were removed with tweezers. Throughout the experiments, the brain was moistened with reptile ringer's solution (in mM: 96.5 NaCl, 31.5 NaHCO<sub>3</sub>, 4 CaCl<sub>2</sub>, 2.6 KCl, 2 MgCl<sub>2</sub> and 20 D-glucose, pH 7.4).

### Experimental setup

Experiments were performed in an air-conditioned laboratory at an ambient temperature of  $21 \pm 2$  °C. A Faraday cage (87 × 70 × 86 cm) was placed on a vibration-isolated table (TMC, LINOS Photomics GmbH, Göttingen, Germany) and covered with light-tight curtain to assure complete darkness. To ensure a background with a constant surface temperature, a pipe system was milled into the back of an aluminum plate (44 × 32 × 1.5 cm) with black plastic lamination attached to its front. Water (temperature 20 °C) was constantly pumped through the pipe system (DC3; K20, Haake-Fisons Instruments, Inc., Saddle Brook, USA) resulting in a surface temperature of  $20 \pm 1$  °C. In all experiments the background temperature was set to 20 °C.

For the experiments, snakes were placed on a styrofoam plate with their head fixed in a custom-built holder (Blum et al. 1978). The center of the receptive field (RF) of a pit organ is slightly shifted up- and sideways with respect to the rattlesnake's long axis (Bakken et al. 2012; Kohl et al.

2012). To line up the center of the RF with the center of the background, the snake's position was shifted 7 cm downwards and 8 cm sideways with respect to the center of the background. The distance between the snake's snout and the uniform thermal background was 16.5 cm. The long axis of the snake was aligned perpendicular to the background plate.

### Electrophysiological recordings

Single- and multi-unit activity was recorded from the optic tectum with microelectrodes pulled (P-87- Brown/Flaming, Sutter Instrument Company, Novato, USA) from borosilicate glass (GB150F-8P, Science Products, Hofheim, Germany) and filled with 2 M NaCl. Electrodes used for single-unit recordings had a resistance of  $\sim 30 \text{ M}\Omega$ . Those used for multi-unit recordings were manually broken at the tip and beveled with a microgrinder (EG-44, Narishige International Limited, London, UK), resulting in a resistance of  $\sim 1 \text{ M}\Omega$ . Electrodes were placed on the surface of the optic tectum contralateral to the stimulated pit organ. A microdrive (SMS 87, TC Elektronik, Zell/Main, Germany) was used to advance the electrode into the brain until neuronal activity was recorded. The signal was amplified and band-pass filtered ( $1000\times$ ; 0.3–3 kHz; DAM 80, World Precision Instruments, Inc., Sarasota, USA). Mains hum (50 Hz) was removed (HumBug, Quest Scientific, Vancouver, Canada) and the signals were digitized (Power 1401, CED, Cambridge, England, sampling rate 40 kHz) and stored on a PC using the software Spike2 (Version 7, CED, Cambridge, England) for offline analysis. Neuronal activity was also displayed on an oscilloscope (PM3335, Philips, Amsterdam, Netherlands) and acoustically monitored using headphones (audio amplifier: TA-AX230, Sony, Tokyo, Japan; headphones: HD 270, Sennheiser, Wedemark-Wennebostel, Germany).

### Stimulation

Pit organs were unilaterally stimulated with an IR emitting object (Fig. 1), which consisted of three Peltier elements ( $4 \times 4 \times 0.4 \text{ cm}$ ; QC-K12705T125, Quick-Ohm Küpper & Co. GmbH, Wuppertal) sandwiched between two vertically orientated aluminum bars ( $5 \times 32 \times 0.5 \text{ cm}$ ). To reduce visual contrast, the front of the object was covered with the same black lamination as the background. Surface temperature of the object was  $35 \text{ }^\circ\text{C}$  and was controlled by means of a Peltier controller unit (PRG H 75, Peltron GmbH Peltier Technik, Fürth, Germany) with a precision of  $\pm 1 \text{ }^\circ\text{C}$ . Since the background had a constant temperature of  $20 \text{ }^\circ\text{C}$ , the resulting thermal contrast was  $15 \text{ }^\circ\text{C}$ . To investigate temperature dependent response characteristics, different surface temperatures of the object (25, 30, 35 and  $40 \text{ }^\circ\text{C}$ )

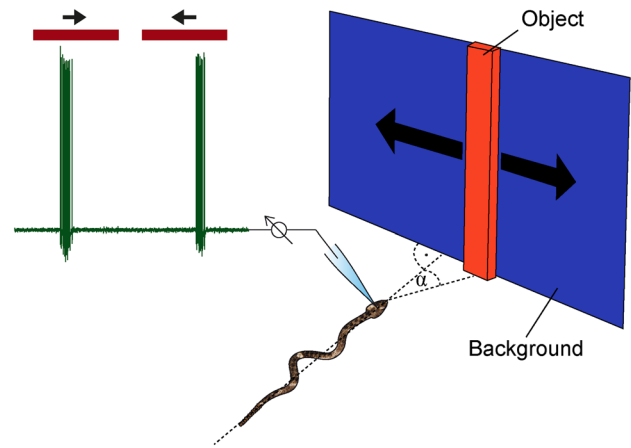


**Fig. 1** Experimental setup. A warm object ( $25\text{--}40 \text{ }^\circ\text{C}$ ) was moved in front of a snake while neuronal activity (green) of an IR-sensitive unit was recorded from the optic tectum. Dark red horizontal bars mark the period when the object was moving (4.9 s). Arrows indicate the direction of movement. The object position  $\alpha$  is the object's angular deviation from the snake's long axis. A temperature controlled aluminum plate ensured a constant and uniform background temperature of  $20 \text{ }^\circ\text{C}$ . Dimensions: object  $5 \times 32 \text{ cm}$ , background  $44 \times 32 \text{ cm}$ , shortest distance from the snout of the snake to the object  $14.5 \text{ cm}$ , respectively,  $16.5 \text{ cm}$  from the snout to the background. Note that the object moved on a linear path perpendicular to the long axis of the snake

were used in one experiment. Thus, the thermal contrast in this experiment varied between  $5$  and  $20 \text{ }^\circ\text{C}$ . A 2-axis plotter (custom-built, Petra Haase Computertechnik, Neuss, Germany) was used to horizontally move the object over a distance of  $36 \text{ cm}$  from left to right and from right to left at a distance of  $2 \text{ cm}$  in front of the background. Note that the object moved perpendicular to the long axis of the snake, resulting in an asymmetric stimulus across the RF of the pit organs. For instance, if the object moved from medial to lateral, the distance between the pit organs and the IR emitting object increased and thus the IR irradiance at the pit organs decreased. Possible consequences of this asymmetry will be discussed. Object position and velocity were controlled and monitored by an AD/DA converter (Power 1401, CED, Cambridge, England) and the software Spike2 (Version 7, CED, Cambridge, England).

### Experimental procedure

At the beginning of each experiment, the setup was illuminated with a white light bulb and the background was covered with a white sheet of paper to provide a search stimulus with sufficient contrast for both the IR and the visual system. The IR object was continually moved from left to right and vice versa at  $90 \text{ mm/s}$  while the microelectrode was advanced in the optic tectum until neuronal activity was encountered. To determine the modality of a

unit (IR or visual + IR), ten stimuli were applied during light and during dark conditions. When a unit responded to IR input (uni- or bimodal), the white sheet of paper was removed and the light was switched off to provide a unimodal IR stimulus. A stimulus was defined as one passage of the object (left–right or right–left). After each stimulus, the object stopped for an inter-stimulus interval of 2 s. A set of two subsequent stimuli of opposite movement direction with the same speed was referred to as a stimulus cycle. Overall, 15 stimulus cycles with different object velocities ranging from 6 to 314 mm/s were presented in a pseudo-random order. The velocities were chosen in regard to the technical limitations of the setup. The entire set of 15 stimulus cycles was repeated five times.

### Data analysis

Signal-to-noise ratio was approx. 5:1 (single-unit recordings) or 3:1 (multi-unit recordings). The mean ongoing activity of a unit was calculated from the number of spikes that occurred during the inter-stimulus intervals. It always was subtracted from the mean number of spikes per stimulus to obtain velocity dependent response functions for each unit. Neuronal activity was calculated separately for both directions of object movement. Stimuli were defined as departing (object movement from nasal to temporal with reference to the stimulated pit organ) and approaching (movement from temporal to nasal) stimuli. A two-sample  $t$  test was used to test, if neuronal activity significantly ( $p < 0.05$ ) differed between departing and approaching stimuli and to determine the directional sensitivity of a unit.

Using the motor signal fed into the 2-axis plotter we calculated the object position for each action potential. The obtained values were called ‘action potential positions’ (depicted as the angular deviation from the snake’s long axis, c.f. Fig. 1). Since each stimulus caused several action potentials, the mean action potential position was calculated from all action potentials and defined as burst position. The mean burst position for a set of approaching and subsequently departing stimuli (same object velocity) was used to define the center of the RF. The standard deviation of the center of the RF at each of the five stimulus repetitions was used as a measure for the precision with which the unit encoded spatial information. Note that a low standard deviation indicates high precision. The precision was calculated separately for each object velocity.

The object velocity was converted to angular velocity  $\omega$  ( $^{\circ}/s$ ). Due to the asymmetry of the stimulus,  $\omega$  was calculated for the center of the RF of a particular unit according to

$$\omega = [(v \times \cos \alpha)/(d/\cos \alpha)] \times 360/2\pi$$

where  $\alpha$  is the angular deviation of the center of the RF from the snake’s long axis in  $^{\circ}$ ,  $v$  is the velocity of the object in mm/s and  $d$  is the shortest distance from the snake’s snout to the object (straight in front of the snake, =145 mm). The term  $360/2\pi$  converts radians to degrees.

To test for bimodal input the neuronal responses during light and dark conditions were compared with a two-sample  $t$  test ( $p < 0.05$ ). Our stimulus paradigm (IR and IR + visual) allowed for a non-ambiguous classification of unimodal IR and bimodal visual depressed IR-sensitive units. Since the temperature of the object was always above background temperature, we could not exclusively stimulate the visual system. Therefore, it was not possible to discriminate bimodal “AND” and unimodal visual units or bimodal “OR” and visual depressed IR units (for definitions see Newman and Hartline 1981).

### Simulation of stimulus and response

The RF of a hypothetical IR-sensitive unit was assumed to conically extent into space with a horizontal angular deviation from the long axis of the snake of  $25^{\circ}$ . The RF size was set to  $60^{\circ}$  to be representative for a tectal IR-sensitive single-unit in crotaline snakes (Terashima and Goris 1976). Given the geometry of our experimental setup, we calculated the solid angle of the RF covered by the stimulating warm object for each object position (c.f. Fig. 7a, black graph). The resulting value was used as a measure for the energy transfer between object and the receptive area of the unit. This was reasonable due to the pinhole camera principle and due to the fact that the center of the pit membrane curvature is near the aperture of the pit. A factor of 0.5 or 2 was multiplied to model cooler or warmer object temperatures. Each object velocity resulted in a different time course of the energy transfer; its derivative (c.f. Fig. 7a, dashed graphs) represents the temperature change rate.

For each object velocity we first estimated the neuronal response to two stimulus parameters individually: (1) The response was assumed to increase with the maximal temperature change rate until saturation (c.f. Fig. 7b, red graphs). (2) The response was assumed to decrease with decreasing exposure time (represented by the reciprocal of the velocity) until saturation (c.f. Fig. 7b, blue graph). The responses were modeled according to logistic functions given by

$$f(x) = L / \left( 1 + e^{-k(x-x_o)} \right)$$

here  $x$  is the maximal temperature change rate, respectively, the exposure time,  $x_o$  is the midpoint of the function,  $L$  is the function’s maximum value (=1) and  $k$  determines the slope. The responses to the two individual parameters (c.f. Fig. 7b, red and blue graphs) were multiplied to simulate

the response to a moving object (c.f. Fig. 7b, green graphs). The input parameters of the logistic functions were arbitrarily adjusted such that the resulting curves resembled the asymmetric response functions observed in the experiments. The input parameters were kept constant across all simulated temperatures.

### Results

We recorded 46 IR and 21 visual single-units. The units were recorded at depths of  $300 \pm 311 \mu\text{m}$  (visual) and  $496 \pm 383 \mu\text{m}$  (IR) relative to the surface of the optic tectum. Only IR single-unit recordings that were stable throughout the entire stimulus protocol were used for further offline analysis ( $n = 20$ ). The average ongoing activity was  $0.025 \pm 0.06 \text{ Hz}$ . All units responded with an increase in spike rate when a warm object passed their RF. Three units decreased their neuronal activity during bimodal stimulation in comparison with the unimodal IR stimulus condition. We thus classified these units as visually depressed IR-sensitive single-units. The remaining units ( $n = 17$ ) were classified as unimodal IR sensitive.

#### Object velocity

The spike rate depended on object velocity. Figure 2a shows the neuronal activity of a representative unit at three object velocities. At the lowest object velocity (2.4°/s) the unit responded with only a few action potentials ( $2.55 \pm 2.95$  spikes/stimulus), even though the object remained within the RF of the unit for the longest period of time. At 29.1°/s, the neuronal activity reached its maximum ( $51.6 \pm 6.2$  spikes/stimulus). Neuronal activity decreased to  $25.9 \pm 2.2$  spikes/stimulus if object velocity was 123.3°/s. The unit showed a steep increase in spike rate between the object velocities 2.4 and 29.1°/s. Spike rates gradually decreased if object velocity was further increased up to 123.3°/s, resulting in an asymmetric response function (Fig. 2b). Although the response functions of different single-units showed variations, the tendency of observing increased activity with an increase in object velocity up to a maximum followed by a slight decrease in activity persisted in the normalized and exponentially fitted data (Fig. 3).

#### Object temperature

Single-unit recordings were not stable long enough to apply a stimulus protocol that allowed for measuring velocity response functions at multiple object temperatures. Therefore, multi-unit recordings were used for this purpose. An increase in object temperature resulted in an increase

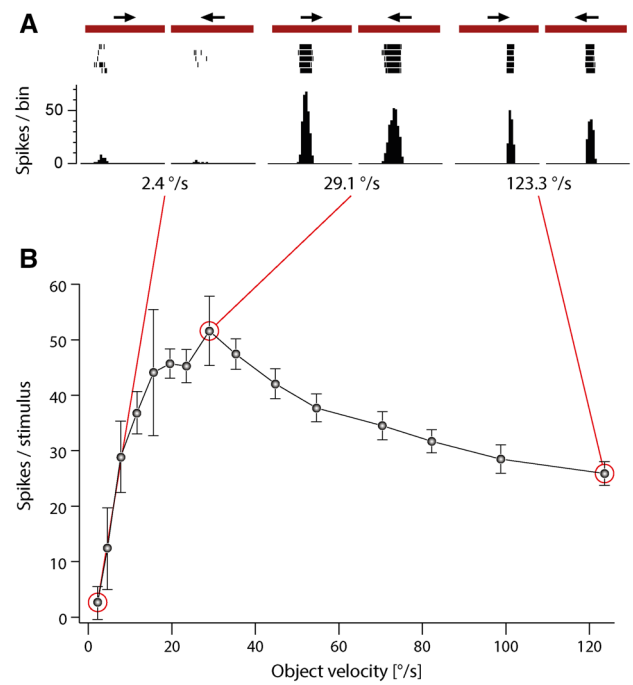


**Fig. 2** Responses of a representative IR-sensitive tectal unit to stimulation with a warm object (35 °C). **a** Raster plots of the responses to 5 stimulus repetitions and corresponding peri-stimulus-time histograms. Object velocity was 2.4, 29.1 and 123.3°/s. Bin width 1.26, 0.16 and 0.08 s. Dark red bars mark the time when the object was moving (60.0, 4.86 and 1.1 s). Black arrows indicate the direction of movement. **b** Neuronal activity as function of object velocity. The mean number of spikes per stimulus (object moving to and fro) was used to quantify neuronal responses. Error bars indicate standard deviation ( $n = 5$ )

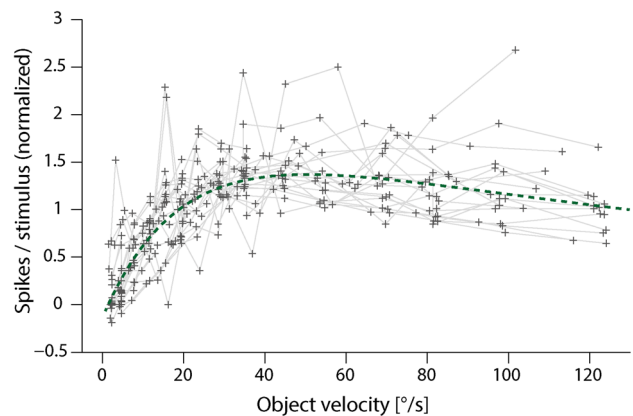


**Fig. 3** Neuronal activity of individual IR units ( $n = 20$ ) as function of object velocity. Dashed line exponential fit across all units. For each unit data were normalized with respect to the average activity across all velocities. Object temperature: 35 °C

of neuronal responses at all object velocities (Fig. 4). The maximum spike rate of each velocity response function increased by a factor of ~8 from 41.9 spikes/stimulus at

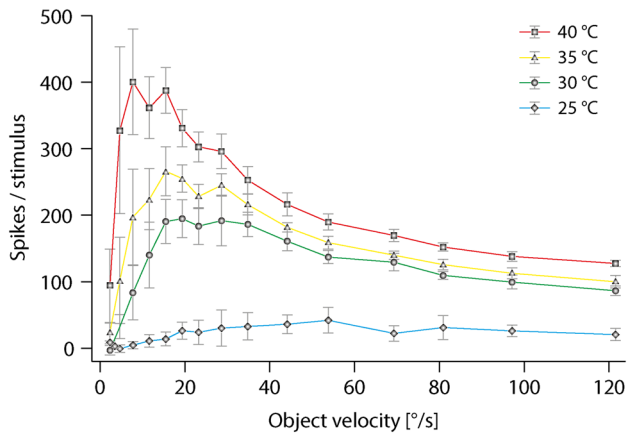


**Fig. 4** Multi-unit activity as function of object velocity and object temperature (25–40 °C). Neuronal activity is expressed as mean number of spikes per stimulus. *Error bars* indicate standard deviation. Each data point is based on 5 stimulus repetitions

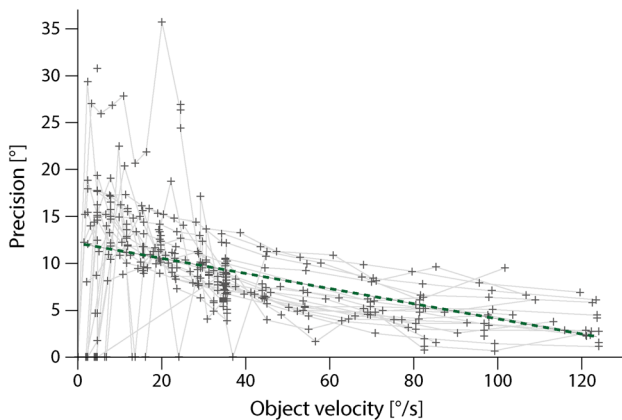


**Fig. 5** Precision of individual IR-sensitive neurons ( $n = 20$ ) as function of object velocity. *Dashed line* linear regression across all units. Note that low values denote a high spatial precision. Object temperature: 35 °C

25 °C to 400.5 spikes/stimulus at 40 °C. In addition, the object velocity at which maximum spike rates were reached shifted from 54.9°/s at 25 °C to 7.9°/s at 40 °C.

### Precision

The precision of single-units increased with increasing object velocities. This is assessed in the raster plots of Fig. 2a (compare the timing of the spikes at object velocities 2.4 and 123.3°/s) and easily observable when the angular precision of all single-units is plotted against object velocity (Fig. 5): the angular deviation across the repetitive stimuli (used as a measure for precision, see materials and methods) decreases from ~15° at low object velocities to ~5° at the highest object velocity.

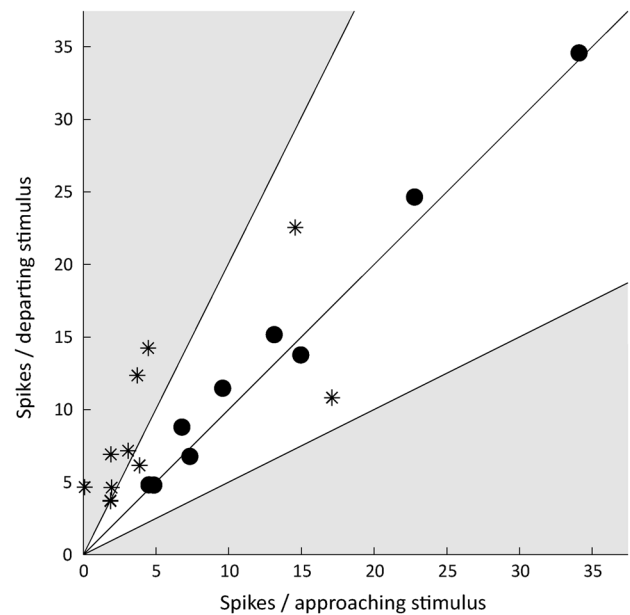


**Fig. 6** Directional sensitivity of IR units ( $n = 20$ ). Neuronal activity in response to a departing stimulus (movement direction corresponds to the side of the stimulated pit organ, object is moving away from the snake) is plotted against the neuronal activity elicited by an approaching stimulus (opposite movement direction). Object temperature was 35 °C. *Solid circles* indicate non-directionally sensitive units, *asterisks* indicate directionally sensitive units (two-sample  $t$  test,  $p < 0.05$ ). *Gray areas* mark units in which neuronal activity was two times stronger for one direction. *Lines* indicate directional response ratios of 2:1, 1:1 and 1:2. The responses of two units were almost identical, resulting in the apparent lack of one data point

### Directional sensitivity

In eleven single-units, neuronal responses to a departing and approaching object differed significantly (Fig. 6). These units were thus classified as directionally sensitive. The neuronal responses of most directionally sensitive units (ten out of eleven) were significantly stronger when the object departed.

## Discussion

### Object velocity

The present study demonstrates that the velocity of a moving IR object is one factor that determines the responses of IR-sensitive tectal units of rattlesnakes. Slowly moving objects elicited weak or no responses. With increasing object velocity the neuronal responses increased up to a maximum and then slightly decreased.

To interpret these results an understanding of the physics of the stimulus is essential. As a warm object moves through the RF of a tectal neuron, the receptive area

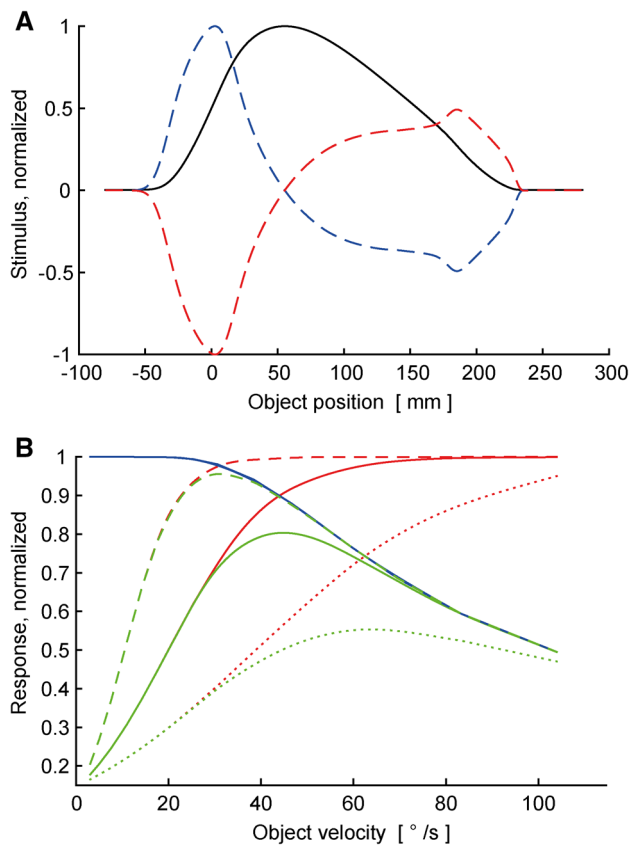


**Fig. 7** Simulation of stimulus and response. **a** The *black curve* indicates the solid angle of the RF covered by the warm object. The *dashed curves* represent the pit membrane temperature change rate for a departing (*blue*) or an approaching (*red*) stimulus. **b** Simulated responses to the individual stimulus parameters exposure time (*blue*) and pit membrane temperature change rate (*red*) and the combined response as present in a moving object stimulus (*green*). *Line style* indicates simulated responses at warmer (*dashed lines*) and cooler (*dotted lines*) object temperatures

(area of the pit membrane that provides input to the neuron, Terashima and Goris 1976) exposed to the IR stimulus gradually increases when the object enters the RF and decreases when the object leaves the RF. The energy transfer between the object and the receptive area (and thus the temperature of the receptive area) is proportional to the part of the receptive area that is exposed to the IR stimulus (c.f. simplified Stefan Boltzmann formula, de Cock Buning 1983).

Besides the membrane area exposed to an IR stimulus, the energy transfer is also influenced by object velocity. A fast moving object should cause a faster change in membrane temperature than a slowly moving object, i.e., it induces a higher temperature change rate (temperature change per time). In contrast, faster moving objects lead to shorter exposure times and hence to a reduction in energy transfer. Overall, a warm moving object leads to a complex IR stimulus. Increasing object velocity results in an

opposing alteration of physical parameters: while the temperature change rate increases, the exposure time and thus the amount of energy transferred decreases.

The responses of sensory units are, however, not only influenced by the physical parameters of the stimulus, but also by the physiological properties of the sensory and nervous system. The IR receptors of crotaline snakes are warmth receptors (de Cock Buning 1981b). They are sensitive to the rate of temperature change, i.e., they respond strongly to high temperature change rates (Bullock and Diecke 1956; de Cock Buning et al. 1981b). Furthermore, peripheral and central nervous recordings have shown that neuronal activity of IR-sensitive cells also decreases with decreasing temperature of the IR emitting object (Bullock and Diecke 1956; Goris and Nomoto 1967; Terashima et al. 1968; Terashima and Goris 1979). Hence, increasing the velocity of an IR object while moving through the RF of a pit organ should lead to competing effects: on the one hand increasing object velocity results in increasing change rates of the membrane temperature and therefore, should lead—until saturation—to an increase of the neuronal response. On the other hand, increasing object velocity leads to shorter exposure times, less energy transfer and thus, to reduced membrane temperatures. This should lead to a decrease in the neuronal response. We suggest that a combination of the contrasting physical properties of our stimulus and the physiological properties of IR-sensitive tectal units lead to the temperature dependent, peak-shaped response functions (Figs. 2b, 3) observed in the presented study.

This assumption is supported by the simulation. Of course, its input parameters were arbitrarily adjusted to obtain the desired response function. Nevertheless, it demonstrates that the asymmetric velocity dependent response function can be modeled by combining the responses to the individual parameters of exposure time and temperature change rate (c.f. Fig. 7b). Given that the membrane temperature change rate increases and the exposure time decreases with increasing object velocity and that both parameters positively correlate with the neuronal response, the maximum response is reached at the velocity at which both parameters are presented in the most efficient ratio.

The results, obtained from tectal recordings, may be significant for the snake's IR detection abilities in general. One could speculate that slow or even stationary objects—as opposed to fast moving objects—may not be detected by the snake at all. Pit vipers are ambush predators that follow a sit and wait strategy (Shine et al. 2002, 2006; Shine and Li-Xin 2002; Eskew et al. 2009). Objects that elicit prey capture behavior usually move and thus stimulate the IR receptors of rattlesnakes. Non-moving objects are usually abiotic, i.e., they are irrelevant to the snake and do not stimulate the IR receptors. Thus, the IR sensory system can

be used by the snakes to separate IR signals from IR background clutter (thermal background).

The results of the present study raise the question of how snakes can detect stationary objects. The ability to do so has been shown in behavioral experiments. Crotaline snakes find suitable places for thermoregulation using their IR system (Krochmal and Bakken 2003). Snakes perform scanning head movements when exposed to IR stimuli (Ebert and Westhoff 2006). We suggest that this behavior creates relative movement between IR objects and the pit membrane and thus enables snakes to detect stationary objects.

The tested object velocities (6–314 mm/s) are within the snake's ecological range: pocket mice of the genus *Perognathus* are one of the main prey animals of *Crotalus atrox* (Beavers 1976). Their maximum running speed is about 275 mm/s (Djawdan 1988). Of course, they often move slower or are stationary. However, the relevant parameter is not the actual speed of the mouse, but its angular velocity with respect to the pit organs. With increasing distance and at a given speed of an IR object, the angular velocity decreases. In addition, the IR irradiance at the pit membrane decreases with increasing distance. In addition, some natural IR objects offer less thermal contrast than in the experiments (35 °C object in front of 20° background). Taking into account all of these factors it can be assumed that many ecologically relevant IR stimuli resemble the critical stimuli of low angular velocities and low thermal contrast (c.f. Fig. 4) used in the present study.

### Object temperature

The multi-unit recordings show that across all object velocities warmer objects elicited stronger responses than cooler objects (c.f. Fig. 4). This is in agreement with previous studies (Bullock and Diecke 1956; de Cock Buning et al. 1981a, 1983) and reflects an increased energy transfer. In addition, with increasing object temperature response peaks shifted towards lower object velocities. We assume that with increasing object temperatures above-threshold temperature change rates are already reached at increasingly lower object velocities. Again, this assumption is supported by the simulation. Altering the object temperatures while keeping the neuronal input parameters constant leads to results similar to the experimental data: Higher object temperatures cause stronger responses and the maximum response is shifted towards lower object velocities.

### Precision

Increasing the object velocity led to an increase in temporal precision (Fig. 5), i.e., a more accurate timing of the neuronal responses with respect to object position. In the present study, the reason for this could have been that with increasing object velocity the temperature change rate also

increased. This effect is not only expected for phasic neurons, but is also of ecological relevance. Crotaline snakes are ambush predators that strike with fast (50–100 ms from initiation of movement to prey contact) deadly bites (Kardong and Bels 1998). A strike must be precisely timed and accurately oriented. Consequently, the ability to precisely localize the prey is indispensable. In addition, faster prey movements require more precise strikes. Our recordings show that the response properties of the IR system of rattlesnakes indeed meet these criteria.

### Directional sensitivity

Specialized directional sensitive neurons have been described for many sensory systems (Heiligenberg and Rose 1987; Marasco and Catania 2007; Wagner and Takahashi 1990; Zittlau et al. 1986). A well investigated example for directional sensitivity is the circuitry of directional sensitive retinal ganglion cells in the visual system of mammals (Borst and Euler 2011). Thus, directional sensitivity can already be computed at an early stage in the pathway of a sensory system. There are only few accounts about directionally sensitive tectal neurons in crotaline snakes (Hartline et al. 1978). Terashima and Goris (1976) searched for directionally sensitive units in the optic tectum of rattlesnakes, but could not confirm their existence. In our study, 50 % of the tectal IR units were directionally sensitive (Fig. 6). It is unknown, to which degree this directional sensitivity is already present at the level of the LTTD and RC or if it is caused by tectal integration mechanisms.

However, due to the linear movement of the object, our IR stimulus was not symmetrical across the RF of the IR organ, due to the continuously increasing distance between object and pit organ while the object moves from nasal to temporal. The irradiance of the receptor decreases with the second power of distance (de Cock Buning 1983) if the angular dimension of the source is smaller than the pit aperture. If the angular dimension of the source exceeds the pit aperture, irradiance varies only with source temperature. Our experimental conditions fall in between: at a distance of 14.5 cm a bar width of 5 cm subtends an angle of about 20°. This is smaller than the horizontal angular dimension of the central field apertures reported by Bakken et al. (2012). In contrast, the vertical dimension of the moving bar exceeds the vertical angular dimension. Consequently, the peak irradiance of the receptor varies as 1/distance and thus decreased from nasal to temporal. Furthermore, the angular velocity of the object—with respect to the pit organ stimulated—decreased from nasal to temporal. In sum, at the nasal edge of the RF the object generated a higher radiation density and had a higher angular velocity than at the temporal edge. Therefore, when the object moves through the RF from temporal to nasal, the temperature change rate



of the pit membrane and thus the neuronal response should be higher, compared to an object moving from temporal to nasal. Surprisingly, ten of the eleven directionally sensitive units responded stronger to a departing than to an approaching object (see materials and methods for definition of movement direction). The RFs of these units were oriented ipsilaterally to the pit organ that provided input to the recording electrode. A departing object crossed the RFs from nasal to temporal and thus caused stronger responses than an approaching object. The RF of the only single-unit that responded stronger to approaching stimuli (c.f. Fig. 6) was, in fact, also the only unit with an RF that was oriented towards the contralateral side. In this case, the RF was crossed from nasal to temporal by an approaching stimulus. Since our results confirm the mechanism described above, the linear movement of the object is most likely responsible for the observed directional sensitivity.

The simulation demonstrates this mechanism as well. Even though the effect of the increasing distance from medial to lateral is neglected, the asymmetry across the RF is evident when the solid angle of the RF covered by the warm object is plotted against object position (Fig. 7a, black curve). The derivative of the curve is taken as a rough estimate of the membrane temperature change rate. It shows that the maximum positive temperature change rate (fastest warming) is higher, when the object moves from medial to lateral (departing stimulus, blue curve) and lower when the object moves in the opposite direction (approaching stimulus, red curve). However, further investigations are needed to empirically support the relevance of the proposed mechanism.

**Acknowledgments** We thank Slawa Braun for animal care and Joachim Mogdans and Vera Schlüssel for critical reading of the manuscript. We also thank two anonymous reviewers for carefully reading and commenting on the manuscript. The authors acknowledge the financial support provided by the DFG (KO4835/1-1). Care and maintenance of experimental animals followed the guidelines for reptiles and venomous snakes. Animal housing and experiments were approved by the LANUVNRW (50.203.2-BN 7, 5/03).

#### Compliance with ethical standards

**Conflict of interest** The authors declare that they have no conflict of interests.

## References

- Bakken GS, Colayori SE, Duong T (2012) Analytical methods for the geometric optics of thermal vision illustrated with four species of pitvipers. *J Exp Biol* 215:2621–2629
- Beavers RA (1976) Food habits of the western diamondback rattlesnake, *Crotalus atrox*, in Texas (Viperidae). *Southwest Nat* 20:503–515
- Blum B, Auker CR, Carpenter DO (1978) A head holder and stereotaxic device for the rattlesnake. *Brain Res Bull* 3:271–274
- Borst A, Euler T (2011) Seeing things in motion: models, circuits, and mechanisms. *Neuron* 71:974–994
- Bullock TH, Diecke F (1956) Properties of an infra-red receptor. *J Physiol* 134:47–87
- Bullock TH, Fox W (1957) The anatomy of the infra-red sense organ in the facial pit of pit vipers. *J Cell Sci* 3:219–234
- Chen Q, Deng H, Brauth SE et al (2012) Reduced performance of prey targeting in pit vipers with contralaterally occluded infrared and visual senses. *PLoS ONE* 7:e34989
- De Cock Buning T (1983) Thresholds of infrared sensitive tectal neurons in *Python reticulatus*, *Boa constrictor* and *Agkistrodon rhodostoma*. *J Comp Physiol A* 151:461–467
- De Cock Buning T, Terashima S, Goris RC (1981a) Crotaline pit organs analyzed as warm receptors. *Cell Mol Neurobiol* 1:69–85
- De Cock Buning T, Terashima S, Goris RC (1981b) Python pit organs analyzed as warm receptors. *Cell Mol Neurobiol* 1:271–278
- Djardjan M (1988) Maximal running speeds of bipedal and quadrupedal rodents. *J Mammal* 69:765–772
- Ebert J, Westhoff G (2006) Behavioural examination of the infrared sensitivity of rattlesnakes (*Crotalus atrox*). *J Comp Physiol A* 192:941–947
- Eskew EA, Willson JD, Winne CT (2009) Ambush site selection and ontogenetic shifts in foraging strategy in a semi-aquatic pit viper, the Eastern cottonmouth. *J Zool* 277:179–186
- Goris RC, Nomoto M (1967) Infrared reception in oriental crotaline snakes. *Comp Biochem Physiol* 23:879–892
- Goris RC, Terashima S (1973) Central response to infra-red stimulation of the pit receptors in a crotaline snake, *Trimeresurus flavoviridis*. *J Exp Biol* 58:59–76
- Gracheva EO, Ingolia NT, Kelly YM et al (2010) Molecular basis of infrared detection by snakes. *Nature* 464:1006–1011
- Gruberg ER, Kicliter E, Newman EA et al (1979) Connections of the tectum of the rattlesnake *Crotalus viridis*: an HRP study. *J Comp Neurol* 188:31–41
- Harris JF, Gamow RI (1971) Snake infrared receptors: thermal or photochemical mechanism? *Science* 172:1252–1253
- Hartline PH, Kass L, Loop MS (1978) Merging of modalities in the optic tectum: infrared and visual integration in rattlesnakes. *Science* 199:1225–1229
- Heiligenberg W, Rose GJ (1987) The optic tectum of the gymnotiform electric fish, *Eigenmannia*: labeling of physiologically identified cells. *Neuroscience* 22:331–340
- Kardong, Bels (1998) Rattlesnake strike behavior: kinematics. *J Exp Biol* 201:837–850
- Kardong KV, Mackessy SP (1991) The strike behavior of a congenitally blind rattlesnake. *J Herpetol* 25:208–211
- Kishida R, Amemiya F, Kusunoki T, Terashima S (1980) A new tectal afferent nucleus of the infrared sensory system in the medulla oblongata of Crotaline snakes. *Brain Res* 195:271–279
- Kohl T, Colayori SE, Westhoff G, Bakken GS, Young BA (2012) Directional sensitivity in the thermal response of the facial pit in western diamondback rattlesnakes (*Crotalus atrox*). *J Exp Biol* 215:2630–2636
- Kohl T, Bothe MS, Luksch H, Straka H, Westhoff G (2014) Organotopic organization of the primary infrared sensitive nucleus (LTTD) in the western diamondback rattlesnake (*Crotalus atrox*). *J Comp Neurol* 522(18):3943–3959
- Krochmal AR, Bakken GS (2003) Thermoregulation in the pits: use of thermal radiation for retreat site selection by rattlesnakes. *J Exp Biol* 206:2539–2545
- Lynn WG (1931) The structure and function of the facial pit of the pit vipers. *Am J Anat* 49:97–139
- Marasco PD, Catania KC (2007) Response properties of primary afferents supplying Eimer's organ. *J Exp Biol* 210:765–780
- Moiseenkova V, Bell B, Motamedi M, Wozniak E, Christensen B (2003) Wide-band spectral tuning of heat receptors in the pit

- organ of the copperhead snake (Crotalinae). *Am J Physiol Integr Comp Physiol* 284:598–606
- Molenaar GJ (1974) An additional trigeminal system in certain snakes possessing infrared receptors. *Brain Res* 78:340–344
- Newman EA, Hartline PH (1981) Integration of visual and infrared information in bimodal neurons in the rattlesnake optic tectum. *Science* 213:789–791
- Newman EA, Gruberg ER, Hartline PH (1980) The infrared trigemino-tectal pathway in the rattlesnake and in the python. *J Comp Neurol* 191:465–477
- Noble GK, Schmidt A (1937) The structure and function of the facial and labial pits of snakes. *Proc Am Phil Soc* 77:263–288
- Schroeder DM, Loop MS (1976) Trigeminal projections in snakes possessing infrared sensitivity. *J Comp Neurol* 169:1–11
- Shine R, Li-Xin S (2002) Arboreal ambush site selection by pit-vipers *Gloydius shedaoensis*. *Anim Behav* 63:565–576
- Shine R, Sun L, Kearney M, Fitzgerald M (2002) Why do Juvenile Chinese pit-vipers (*Gloydius shedaoensis*) select arboreal ambush sites? *Ethology* 108:897–910
- Shine R, Sun L, Kearney M, Fitzgerald M (2006) Thermal correlates of foraging-site selection by Chinese pit-vipers (*Gloydius shedaoensis*, Viperidae). *J Therm Biol* 27:405–412
- Terashima S, Goris RC (1976) Receptive area of an infrared tectal unit. *Brain Res* 101:155–159
- Terashima S, Goris RC (1979) Receptive areas of primary infrared afferent neurons in crotaline snakes. *Neuroscience* 4:1137–1144
- Terashima S, Goris RC, Katsuki Y (1968) Generator potential of crotaline snake infrared receptor. *J Neurophysiol* 31:682–688
- Van Dyke JU, Grace MS (2010) The role of thermal contrast in infrared-based defensive targeting by the copperhead, *Agkistrodon contortrix*. *Anim Behav* 79:993–999
- Wagner H, Takahashi T (1990) Neurons in the midbrain of the barn owl are sensitive to the direction of apparent acoustic motion. *Naturwissenschaften* 77:439–442
- Zittlau KE, Class B, Münz H (1986) Directional sensitivity of lateral line units in the clawed toad *Xenopus laevis* Daudin. *J Comp Physiol A* 158:469–477